



**ARTICLE**

# Performance Prediction of an Optimized Centrifugal Pump with High Efficiency

Yuqin Wang<sup>1,2,3,\*</sup>, Luxiang Zhou<sup>3</sup>, Mengle Han<sup>1</sup> and Lixiang Shen<sup>1</sup>

<sup>1</sup>School of Mechanical Engineering, Chaohu University, Chaohu, 238024, China

<sup>2</sup>College of Engineering, Technological University of the Philippines, Manila, 1106, Philippines

<sup>3</sup>School of Mechanical Engineering, Anhui Polytechnic University, Wuhu, 241000, China

\*Corresponding Author: Yuqin Wang. Email: wyqlll@126.com

Received: 18 October 2022 Accepted: 19 January 2023 Published: 18 May 2023

## ABSTRACT

The main structural parameters of the IR100-80-100A type chemical centrifugal pump have been optimized by means of an orthogonal test approach. The centrifugal pump has been modeled using the CFturbo software, and 16 sets of orthogonal-test schemes have been defined on the basis of 4 parameters, namely, the blade number, blade outlet angle, impeller outlet diameter, and impeller outlet width. Such analysis has been used to determine the influence of each index parameter on the pump working efficiency and identify a set of optimal combinations of such parameters. The internal flow field in the centrifugal pump has been simulated by using the Pumplinx software. These numerical results have shown that, compared with the prototype pump, the outlet pressure and shaft power of the optimized pump can be significantly reduced, and the pump working efficiency can be improved by 5.59%. In the present study, some arguments are also provided to demonstrate that, with respect to other optimization methods, the orthogonal test approach is more convenient, and requires less test times.

## KEYWORDS

Centrifugal pump; structural design; work efficiency; internal flow field simulation; impeller

## 1 Introduction

The first to propose the concept of the centrifugal pump was the French engineer Papin, he made the world's first centrifugal pump for lifting liquids in 1705. Due to its simple structure, low production cost and wear resistance, the centrifugal pump, which is used for energy conversion, is widely used in various fields [1–5]. However, in the energy conversion process of the centrifugal pump, various energy losses are inevitably generated, resulting in the low working efficiency of the pump. How to improve the pump working efficiency has become a key research direction for the majority of researchers and manufacturers. At present, many experts and scholars are committed to studying how to reduce energy loss and improve pump efficiency in the working process, and have achieved certain results. Li et al. [6] used the crowd search algorithm to optimize the blade structure parameters, and obtained the optimal parameter combination, which improved the working efficiency of the centrifugal pump. He et al. [7] used the response surface method to fit the impeller structural parameters, head and efficiency, and obtained the best combination of multiple factors, which significantly improved the efficiency of the centrifugal pump. Xing et al. [8] obtained better impeller structure parameters based on the Box-Behnken simulation test platform with no-load wind speed as the indicator. Sun [9] used the Pro/Mechanica to design a



lightweight impeller model, reducing the impeller mass and saving costs. Hoseinib et al. [10] used the multi-objective genetic algorithm to optimize the design of impeller parameters, reducing the power consumption of centrifugal pumps. Adiaconitei et al. [11] used additive manufacturing technology to design an impeller, which improved the surface accuracy of the impeller.

To improve the working efficiency of a centrifugal pump and reduce power consumption, the orthogonal test method will be used to optimize the main parameters of the pump to obtain better impeller combination parameters. In this paper, the relevant structural parameters of the centrifugal pump will be calculated, the CFTurbo software will be used to model the centrifugal pump, and the internal flow field will be simulated based on PumLinx software. Finally, through orthogonal test and range analysis, the optimal combination of impeller structural parameters will be obtained, so as to improve the centrifugal pump's working efficiency in use and reduce the use cost.

## 2 Design of the Main Structural Parameters of Centrifugal Pump

The IR100-80-100A type chemical centrifugal pump is selected as the prototype pump, as shown in Fig. 1. The basic parameters of the prototype pump are:  $Q = 59 \text{ m}^3/\text{h}$ ; head  $H = 100 \text{ m}$ ; and rotational speed  $n = 2900 \text{ r/min}$ .

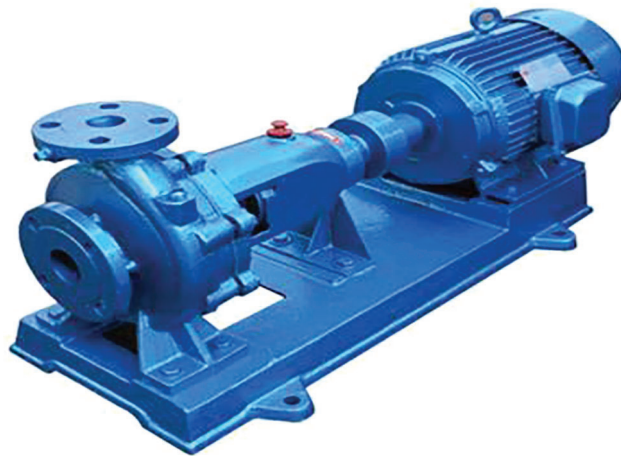


**Figure 1:** IR100-80-100A type chemical centrifugal pump

To improve the calculation accuracy, the variation range of the main structural parameters of the centrifugal pump impeller is restricted. The restriction conditions for each performance parameter are given in Eq. (1) [12].

$$\left\{ \begin{array}{l} 3.5 \sqrt[3]{\frac{Q}{n}} < D_1 < 5.5 \sqrt[3]{\frac{Q}{n}} \\ 9.35 \left(\frac{n_s}{100}\right)^{-\frac{1}{2}} \sqrt[3]{\frac{Q}{n}} < D_2 < 10.5 \left(\frac{n_s}{100}\right)^{-\frac{1}{2}} \sqrt[3]{\frac{Q}{n}} \\ 0.64 \left(\frac{n_s}{100}\right)^{\frac{5}{6}} \sqrt[3]{\frac{Q}{n}} < b_2 < 0.8 \left(\frac{n_s}{100}\right)^{\frac{5}{6}} \sqrt[3]{\frac{Q}{n}} \\ 23^\circ < \beta_1 < 40^\circ \\ 22^\circ < \beta_2 < 30^\circ \\ 3 < Z < 8 \\ 90^\circ < \varphi < 130^\circ \end{array} \right. \quad (1)$$

In Eq. (1),  $D_1$  is the impeller inlet diameter,  $D_2$  is the impeller outlet diameter,  $n_s$  is the specific speed,  $b_2$  is the impeller outlet width,  $\beta_1$  is the blade inlet angle,  $\beta_2$  is the blade outlet angle,  $Z$  is the blade number, and  $\varphi$  is the blade wrap angle.

The main structural parameters of the centrifugal pump impeller are calculated by the velocity coefficient method [6], as presented in Table 1.

**Table 1:** Main structural parameters of the impeller

Parameters	Results
Impeller inlet diameter, $D_1$ /mm	75.13
Impeller outlet diameter, $D_2$ /mm	264.87
Impeller outlet width, $b_2$ /mm	8.8
Blade inlet angle, $\beta_1/^\circ$	27
Blade outlet angle, $\beta_2/^\circ$	29
Blade thickness, $S$ /mm	3
Blade number, $Z$	5
Blade wrap angle, $\varphi/^\circ$	120

### 3 Orthogonal Test Plan Design

The system performance will be restricted by many factors, and to clarify the influence sequence of various factors on the system, relevant tests are needed. The traditional permutation and combination method needs to test all combinations of the various factors, but the number of tests is numerous and the workload of tests is large. To reduce the number of trials and workload, mathematicians have developed a new test method—the orthogonal test. The method of the orthogonal test is to establish an orthogonal test table by selecting some representative factors, and carrying out statistical analysis, overall design, and comprehensive comparison to obtain the horizontal combination which is closest to the best scheme [7–9]. The orthogonal test only selects some factors to carry out the test and does not consider the arrangement and combination of all factors, thus improving the test efficiency. It is a fast and convenient method of optimization.

Considering the influence of various factors on the centrifugal pump efficiency, 4 parameters including the blade number  $Z$ , the blade outlet angle  $\beta_2$ , the impeller outlet diameter  $D_2$  and the impeller outlet width  $b_2$ , are selected as the test factors. The orthogonal test table is established as shown in Table 2, and each test factor is set at 4 levels.

**Table 2:** Orthogonal test table

Levels	Factors			
	$A$ $Z$	$B$ $\beta_2/^\circ$	$C$ $D_2$ /mm	$D$ $b_2$ /mm
1	4	27	250	7
2	5	28	260	8
3	6	29	270	9
4	7	30	280	10

According to the  $L_{16}(4^4)$  test table, 16 groups of orthogonal test schemes with 4 levels and 4 factors are set up, as shown in [Table 3](#).

**Table 3:** Orthogonal test schemes

Serial numbers	Test factors				Corresponding parameters			
	<i>A</i>	<i>B</i>	<i>C</i>	<i>D</i>	<i>Z</i>	$\beta_2/^\circ$	$D_2/\text{mm}$	$b_2/\text{mm}$
1	$A_1$	$B_1$	$C_1$	$D_1$	4	27	250	7
2	$A_1$	$B_2$	$C_2$	$D_2$	4	28	260	8
3	$A_1$	$B_3$	$C_3$	$D_3$	4	29	270	9
4	$A_1$	$B_4$	$C_4$	$D_4$	4	30	280	10
5	$A_2$	$B_1$	$C_2$	$D_3$	5	27	260	9
6	$A_2$	$B_2$	$C_1$	$D_4$	5	28	250	10
7	$A_2$	$B_3$	$C_4$	$D_1$	5	29	280	7
8	$A_2$	$B_4$	$C_3$	$D_2$	5	30	270	8
9	$A_3$	$B_1$	$C_3$	$D_4$	6	27	270	10
10	$A_3$	$B_2$	$C_3$	$D_3$	6	28	280	9
11	$A_3$	$B_3$	$C_1$	$D_2$	6	29	250	8
12	$A_3$	$B_4$	$C_2$	$D_1$	6	30	260	7
13	$A_4$	$B_1$	$C_4$	$D_2$	7	27	280	8
14	$A_4$	$B_2$	$C_3$	$D_1$	7	28	270	7
15	$A_4$	$B_3$	$C_2$	$D_4$	7	29	260	10
16	$A_4$	$B_4$	$C_1$	$D_3$	7	30	250	9

## 4 Simulation and Analysis of Internal Flow Field

### 4.1 Grid Division

PumpLinx is a hydraulic simulation software specifically designed for fluid mechanical analysis, which can accurately simulate fluid flow and cavitation, etc. [10–12]. The built three-dimensional model of the centrifugal pump is imported into PumpLinx software and the Cartesian grid is divided, as shown in [Fig. 2](#).

Because the grid number of centrifugal pump has a great influence on the experimental results, grid independence analysis is required. Taking the outlet pressure and head of the volute as the index, the influence of different grid numbers on the index is considered. The grid independence analysis results are shown in [Table 4](#).

As can be seen from [Table 4](#), when the number of grids is 2,356,897, each index has reached a stable state, and the working performance of the system is stable. After comprehensive consideration, the number of grids is determined to be 2,356,897.

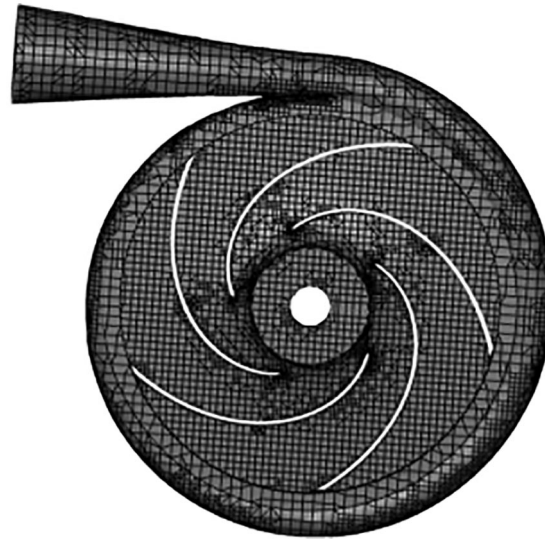


**Figure 2:** Centrifugal pump grid division

**Table 4:** Grid independence analysis of centrifugal pump

Grid number	Volute outlet pressure/Pa	Head/m
965324	425687	47.65
2356897	432412	42.36
4505546	446523	42.85
5678544	448752	43.12

#### 4.2 Boundary Condition Setting

The boundary conditions mainly include the import boundary condition, export boundary condition, wall boundary condition, and interface boundary condition. The selection criteria of the turbulence model mainly include whether the fluid is compressible, establishing special feasible problems, accuracy requirements, computer capabilities, and time constraints. Turbulence model calculation methods mainly include Reynolds time average simulation, scale analytical simulation, and direct numerical simulation. Among them, the  $k - \varepsilon$  model in Reynolds time averaged simulation has the advantages of wide application, economy, and reasonable accuracy. The  $k - \varepsilon$  model is derived from the transient  $N - S$  equation [13]. The  $k - \varepsilon$  model is applied to the turbulence model, and the inlet velocity distribution is uniform.

The Reynolds time average  $N - S$  continuous equation is [14]:

$$\frac{\partial \rho}{\partial t} + \frac{\partial}{\partial x_i} (\rho u_i) = 0 \quad (2)$$

In Eq. (2),  $u_i$  is the Reynolds mean velocity component with the mean sign omitted, and  $\rho$  is the density.

The Reynolds time averaged  $N - S$  momentum equation is [15]:

$$\frac{\partial}{\partial t} (\rho u_i) + \frac{\partial}{\partial x_j} (\rho u_i u_j) = -\frac{\partial p}{\partial x_i} + \frac{\partial \sigma_{ij}}{\partial x_j} + \frac{\partial}{\partial x_j} (-\rho u' i u' j) \quad (3)$$

In Eq. (3),  $p$  is the pressure,  $u'_i$  is the pulsating velocity,  $x_i$  is the coordinate component, and  $\sigma_{ij}$  is the stress tensor component.

Using the quality exit boundary condition, there is no slippage on each solid wall surface. The interface between the inlet and impeller and between the impeller and volute shall be the interface between the dynamic and static coupling platform [16].

The finite volume method is used to discretize the control equation [17]. The second order fully implicit scheme is used to discretize the time term [18]. The diffusion term and pressure term are discretized by the central difference scheme [19]. Second-order upwind scheme is adopted for convection term [20]. And the pressure and velocity equations are solved by full coupling technique [21].

Assuming that the fluid medium inside the centrifugal pump is an incompressible Newtonian fluid, and the fluid medium is water, its basic properties are given in Table 5 [22].

**Table 5:** Basic property settings of fluid medium

Parameters	Parameter values
Reference temperature	20°C
Standard atmospheric pressure	101325 Pa
Fluid density	998 kg/m <sup>3</sup>
Saturated vapor pressure	3610 Pa
Kinematic viscosity	1 × 10 <sup>-6</sup> m <sup>2</sup> /s
Vapor density	0.0245 kg/m <sup>3</sup>

### 4.3 Orthogonal Test Results

According to the orthogonal test schemes in Table 3, 16 different centrifugal pump models were established [23]. The internal flow field simulation was performed by using PumpLinx software to obtain the corresponding shaft power, outlet pressure and inlet pressure of the pump. The head and efficiency of the centrifugal pump were calculated by Eq. (4), and the obtained results are presented in Table 6.

$$\left\{ \begin{array}{l} H = \frac{P_1 - P_2}{\rho g} \\ \eta = \frac{\rho g Q H}{P} \\ P = \frac{\rho g Q H}{1000 \eta} \end{array} \right. \quad (4)$$

**Table 6:** Orthogonal test results for pump inlet and outlet pressures, fluid density, and pump shaft power

Test serial numbers	$P/W$	$P_1/\text{Pa}$	$P_2/\text{Pa}$	$H/\text{m}$	$\eta/\%$
1	12875.5	706977	101325	61.80122	75.26
2	15508.7	801512	101325	71.44765	72.23
3	18071.7	894768	101325	80.96357	70.24
4	22498.3	983261	101325	89.99347	62.72

(Continued)

Table 6 (continued)					
Test serial numbers	$P/W$	$P_1/\text{Pa}$	$P_2/\text{Pa}$	$H/\text{m}$	$\eta/\%$
5	17427.5	875282	101325	78.9752	71.05
6	16582.5	836143	101325	74.98143	70.90
7	19244.8	978678	101325	89.52582	72.94
8	18736.6	936477	101325	85.21959	71.31
9	21787.4	1009800	101325	92.70153	66.71
10	22850.2	1061420	101325	97.96888	67.22
11	15987.3	821643	101325	73.50184	72.08
12	16880.8	870771	101325	78.5149	72.92
13	25577.1	1012470	101325	92.97398	56.99
14	19779.8	993696	101325	91.05827	72.18
15	21257.9	978660	101325	89.52398	66.03
16	33251.2	976335	101325	89.28673	42.10

In Eq. (4),  $P_1$  is the pump outlet pressure,  $P_2$  is the pump inlet pressure,  $\rho$  is the fluid density, and  $P$  is the pump shaft power.

#### 4.4 Range Analysis

The range analysis method, also known as the intuitive analysis method, is the most commonly used method of analysis of orthogonal test results, and it has the advantages of simple calculation, intuitive image, is simple and easy to understand, etc., Eq. (5) is a range method analysis and calculation formula. The results of the orthogonal test are analyzed by Eq. (5), and the order of influence of each parameter on the centrifugal pump efficiency is obtained [24].

$$\begin{cases} K_i = \sum_{i=1}^4 E_i \\ k_i = \frac{1}{4} \sum_{i=1}^4 E_i \\ R = k_{i\max} - k_{i\min} \end{cases} \quad (5)$$

In Eq. (5),  $K_i$  is the sum of the simulation results in PumpLinx software for the same factors in the orthogonal test data.  $E_i$  is the value of a certain indicator.  $k_i$  is the average of the simulation results in PumpLinx software for the same factors in the orthogonal test data.  $R$  is the range, that is, the difference between the maximum and minimum values of the average of the simulation results in PumpLinx software for the same factor in the orthogonal test data. In general, the size of  $k_i$  can determine the optimal level of  $i$  factors and the optimal level combination of all factors, that is, the optimal combination. The larger the  $R$ , the greater the influence of the factor on the system performance. According to the size of  $R$ , the primary and secondary factors can be determined [25].

The range calculation was performed on the orthogonal test results of the centrifugal pump by Eq. (5), and the calculation results are presented in Table 7.

**Table 7:** Analysis of influence of various parameters on the pump working efficiency

Parameters	Influence factors			
	<i>A</i>	<i>B</i>	<i>C</i>	<i>D</i>
$K_1$	2.8045	2.7001	2.6034	2.933
$K_2$	2.862	2.8303	2.8825	2.7261
$K_3$	2.7893	2.8129	2.8044	2.5061
$K_4$	2.373	2.4905	2.5987	2.6636
$k_1$	0.7011	0.6750	0.6509	0.7333
$k_2$	0.7155	0.7076	0.7056	0.6815
$k_3$	0.6973	0.7032	0.7011	0.6265
$k_4$	0.5933	0.6223	0.6497	0.6659
$R$	0.1222	0.0853	0.0559	0.1068
Sorting	1	3	4	2

As can be seen from Table 7, the order of the degree influence of the selected parameters on the centrifugal pump working efficiency is *ADBC*. Taking the optimum working efficiency of centrifugal pump as the evaluation criterion, the optimum combination is  $A_2B_2C_2D_1$ , namely,  $Z = 5$ ,  $\beta_2 = 28^\circ$ ,  $D_2 = 260$  mm,  $b_2 = 7$  mm.

#### 4.5 Simulation of Internal Flow Field in Centrifugal Pump

To verify the feasibility of the orthogonal test optimization scheme, the internal flow field simulations are carried out on the prototype pump and the optimized pump at a rated speed ( $n_d = 2900$  r/min), and the simulation results are shown in Figs. 3 and 4, respectively.

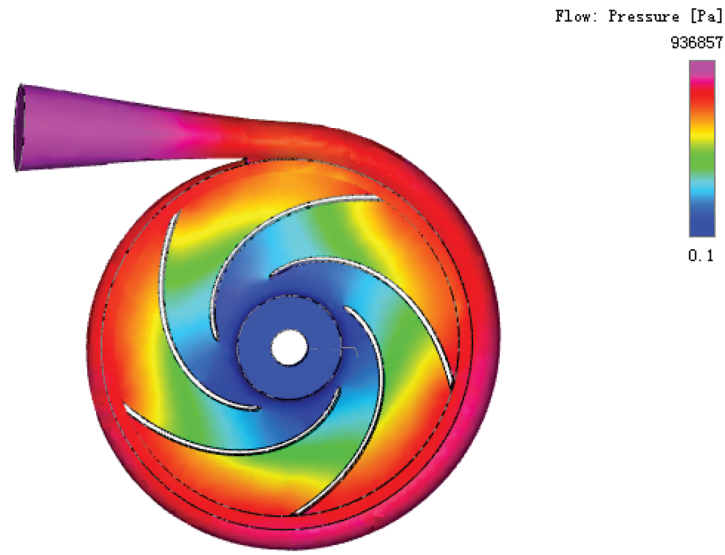
As can be seen from Figs. 3 and 4, the centrifugal pump outlet pressure before optimization is 936857 Pa, and the pump shaft power is 18668.7 W. The optimized centrifugal pump outlet pressure is 832275 Pa and the pump shaft power is 15493.1 W. Combined with Eq. (2), the centrifugal pump working efficiency before and after optimization can be calculated to be 73.3% and 77.4%, respectively, which means that the working efficiency is increased by 5.59%.

### 5 Verification and Analysis of External Characteristic Test

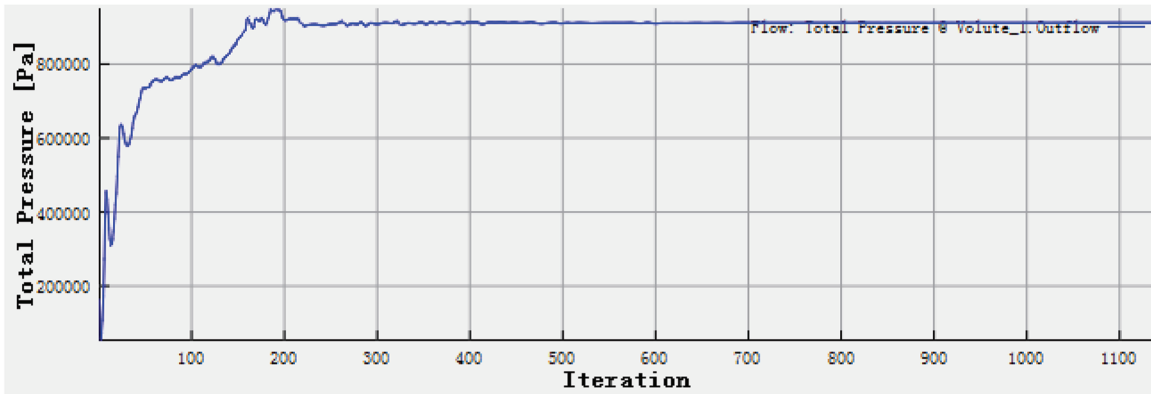
To verify the correctness of the optimization scheme, the IR100-80-100A type chemical centrifugal pump is selected to build the external characteristic test platform. The impeller is made based on the optimal combination parameters. The impeller material is polylactic acid (PLA), as shown in Fig. 5.

The external characteristics of the prototype pump and the optimized pump are tested by CFD technology. The flow rate of the working conditions are  $0.1Q_d$ ,  $0.3Q_d$ ,  $0.5Q_d$ ,  $0.7Q_d$ ,  $0.9Q_d$  and  $1.1Q_d$ , respectively (where, the rated flow rate  $Q_d = 59$  m<sup>3</sup>/h). The test results are shown in Fig. 6.

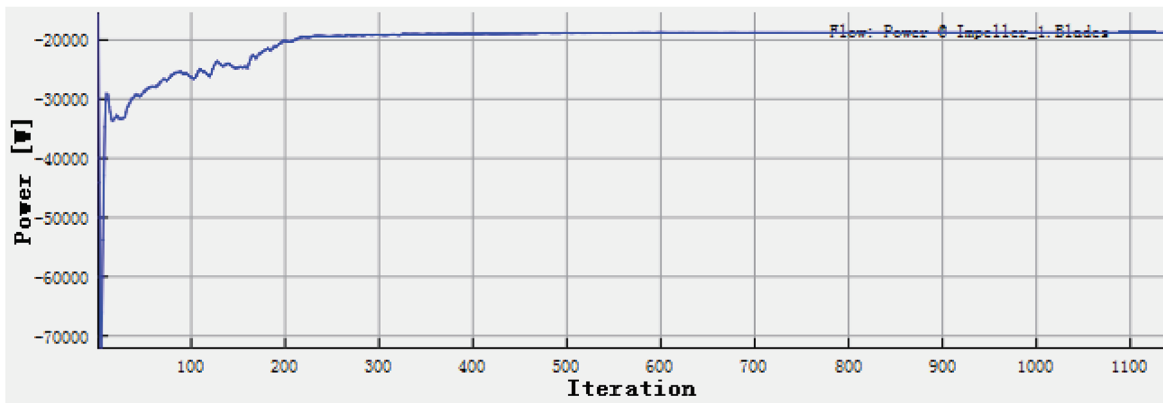
As can be seen from Fig. 6, with the increase of flow rate, the centrifugal pump working efficiency gradually increases, reaching the maximum value near the rated flow rate. The change trend of the working efficiency curve of the optimized pump and the prototype pump is basically the same, and the change law can be clearly expressed.



(a) Prototype pump internal flow field pressure cloud map

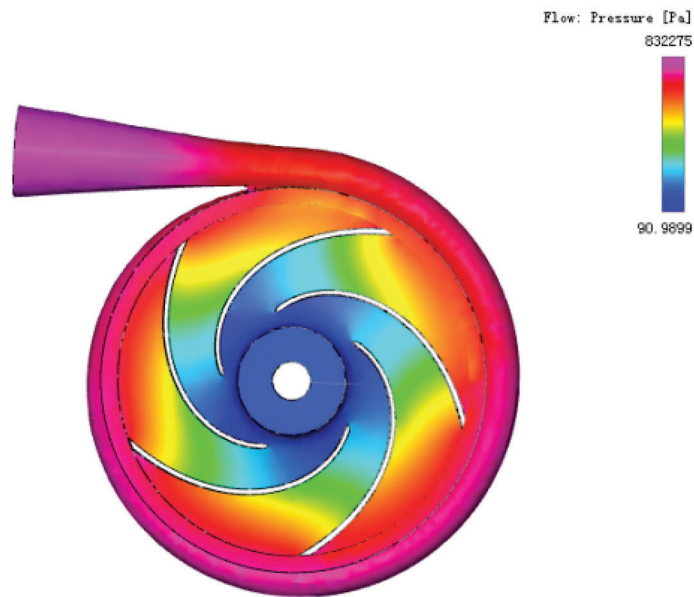


(b) Prototype pump outlet pressure curve

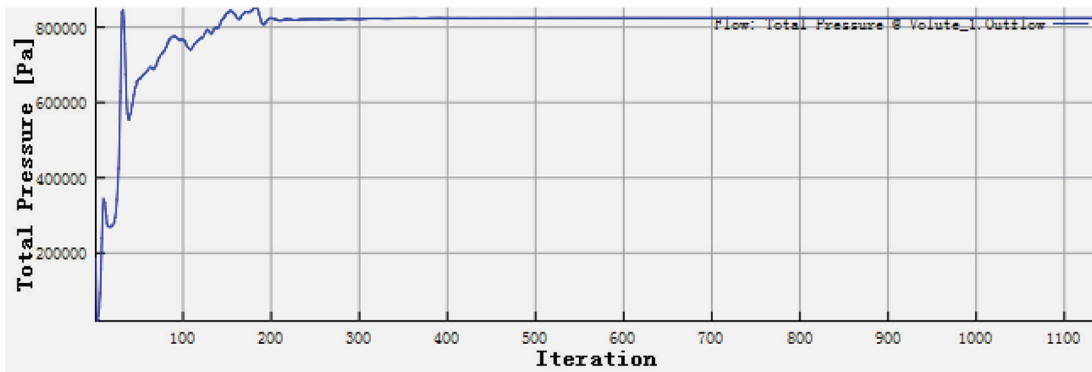


(c) Prototype pump shaft power curve

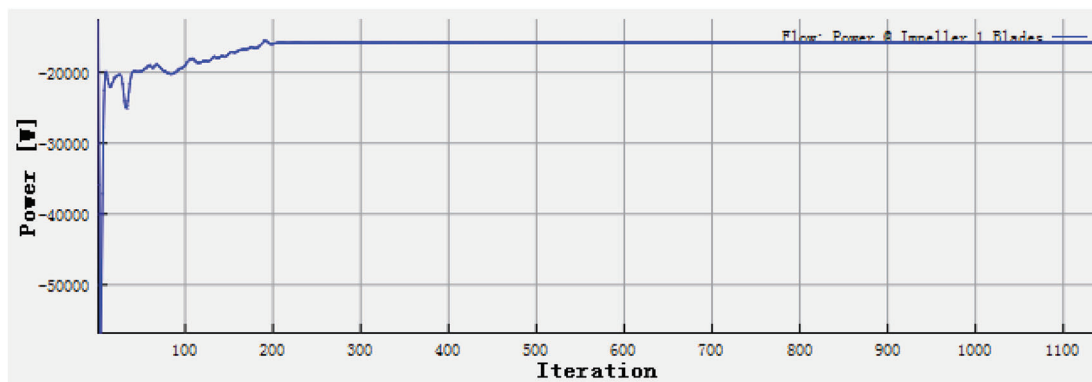
**Figure 3:** Simulation results of the prototype pump internal flow field



(a) Optimized pump internal flow field pressure cloud map



(b) Optimized pump outlet pressure curve



(c) Optimized pump shaft power curve

**Figure 4:** Simulation results of the optimized pump internal flow field



**Figure 5:** Optimized pump impeller

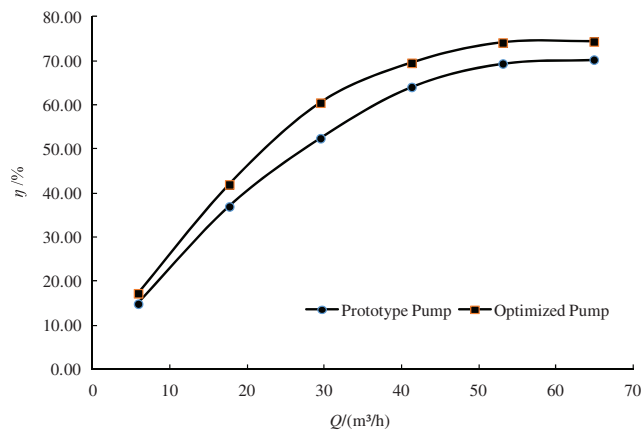


**Figure 6:** Comparison of external characteristics of the prototype pump and optimized pump

The pump working efficiency under different operating conditions is extracted from Fig. 6, and presented in Table 8.

**Table 8:** Test results of the working efficiencies of the centrifugal pump under different operating conditions

Indexes	$0.1Q_d$	$0.3Q_d$	$0.5Q_d$	$0.7Q_d$	$0.9Q_d$	$1.1Q_d$
Prototype pump $\eta$ /%	14.88	36.94	52.41	64.04	69.35	70.20
Optimized pump $\eta$ /%	17.26	41.93	60.46	69.50	74.10	74.35
$\Delta\eta$ /%	15.99	13.51	15.36	8.53	6.85	5.87

From Table 8, the optimized value of the pump working efficiency under different working conditions is greater than the prototype pump value, and the performance is improved significantly, achieving the expected optimization goal. The main reason for this is that the three structural parameters of optimized pump blade

outlet angle, impeller outlet diameter, and impeller outlet width are all reduced, which reduces wear on the surfaces of the impeller and guide vanes, reduces hydraulic losses, improves the efficiency of fluid flow, and thus improves the centrifugal pump's working efficiency. The accuracy of the optimization method of centrifugal pump efficiency based on orthogonal test is further verified through the external characteristic test of centrifugal pump working efficiency.

## 6 Summary

- (1) The IR 100-80-100A type chemical centrifugal pump was selected as the prototype pump, and the mathematical model with the optimal pump working efficiency as its objective function was established. The main structural parameters of the impeller were optimized by orthogonal test. The order of degree of influence of the main structural parameters of the centrifugal pump on the pump working efficiency was obtained through range analysis and calculation, and a set of optimal combination parameters was obtained.
- (2) The internal flow field simulation of the prototype pump and the optimized pump was carried out by using PumpLinx software. The simulation results showed that the outlet pressure and shaft power of the optimized pump had both decreased significantly, and the pump working efficiency had increased by 5.59%, which verified the feasibility of the orthogonal test optimization scheme.
- (3) The external characteristic test platform of the centrifugal pump was built and the optimized pump impeller was made. The external characteristic test results showed that the optimized pump working efficiency under different working conditions was greater than the prototype pump value, and the system performance was improved obviously, which further verified the accuracy of the orthogonal test scheme.
- (4) Taking the centrifugal pump as the research object, the orthogonal design and range analysis were used to optimize the main structural parameters of the pump, which improved the pump working efficiency. Based on the external characteristic test bench, the accuracy of the optimization method was verified. In the next step, the multi-objective optimization design method of centrifugal pump will be focused on to comprehensively improve the centrifugal pump's hydraulic performance.

**Funding Statement:** This project is supported by the Anhui Province University Discipline (Professional) Top Talent Academic Funding Project (No. gxbjZD2021076). This project is supported by the Key Project of Natural Science Research in Colleges and Universities of Anhui Province (No. KJ2021A1026). This project is supported by the Key Project of Natural Science Foundation of Chaohu University (No. XLZ-201902).

**Author Contributions:** Y. W.: Structure Design, Algorithm Design; M. H.: Drawing Graphics; L. S.: Experiment. All authors have read and agreed to the published version of the manuscript.

**Conflicts of Interest:** The authors declare that they have no conflicts of interest to report regarding the present study.

## References

1. Wang, W. J., Yuan, S. Q., Pei, J., Zhang, J. F., Yuan, J. P. et al. (2015). Two-point hydraulic optimization of pump impeller based on kriging model and neighborhood cultivation genetic algorithm. *Journal of Mechanical Engineering*, 51(15), 33–38. <https://doi.org/10.3901/JME.2015.15.033>
2. Tan, L., Cao, S., Wang, Y., Zhu, B. (2012). Direct and inverse iterative design method for centrifugal pump impellers. *Proceedings of the Institution of Mechanical Engineers, Part A: Journal of Power and Energy*, 226(6), 764–775. <https://doi.org/10.1177/0957650912451411>

3. Kim, S., Choi, Y. S., Lee, K. Y., Yoon, J. Y. (2009). Design optimization of centrifugal pump impellers in a fixed meridional geometry using DOE. *International Journal of Fluid Machinery & Systems*, 2(2), 172–178. <https://doi.org/10.5293/IJFMS.2009.2.2.172>
4. Sakthivel, N. R., Sugumaran, V., Nair, B. B. (2012). Automatic rule learning using roughset for fuzzy classifier in fault categorization of mono-block centrifugal pump. *Applied Soft Computing*, 12(1), 196–203. <https://doi.org/10.1016/j.asoc.2011.08.053>
5. Derakhshan, S., Pourmahdavi, M., Abdollahnejad, E., Reihani, A., Ojaghi, A. (2013). Numerical shape optimization of a centrifugal pump impeller using artificial bee colony algorithm. *Computers & Fluids*, 81(9), 145–151. <https://doi.org/10.1016/j.compfluid.2013.04.018>
6. Li, Y. L., Sun, X. W., Yang, H. R., Wang, H. Y., Liu, Y. et al. (2022). Optimization of impeller structure parameters of cementing mud flowmeter based on response surface and crowd search algorithm. *Journal of Electronic Measurement and Instrumentation*, 36(5), 12–20.
7. He, K. J., Heng, Y. G., Zhang, W. B., Jiang, Q. F. (2021). Research on optimization of disc pump impeller based on response surface method. *Journal of Engineering for Thermal Energy and Power*, 36(8), 8–15.
8. Xing, H. N., Ma, S. C., Mo, J. L., Zeng, B. S., Liang, W. P. et al. (2021). Optimization and experiment of parameters for the impeller structure of extractor in a sugarcane chopper harvester. *Transactions of the Chinese Society of Agricultural Engineering*, 37(12), 12–19.
9. Sun, W. (2020). Design optimization of impeller structure of liquid ring vacuum pump: A simulation study. *Chinese Journal of Vacuum Science and Technology*, 40(5), 395–399.
10. Hoseini, S. S., Najafi, G., Ghobadian, B., Akbarzadeh, A. H. (2021). Impeller shape-optimization of stirred-tank reactor: CFD and fluid structure interaction analyses. *Chemical Engineering Journal*, 413(1), 2–18. <https://doi.org/10.1016/j.cej.2020.127497>
11. Adiaconitei, A., Vintila, I. S., Mihalache, R., Paraschiv, A., Frigioescu, T. F. et al. (2021). Manufacturing of closed impeller for mechanically pump fluid loop systems using selective laser melting additive manufacturing technology. *Materials*, 14(20), 1–17.
12. Wang, Y. Q., Huo, X. W., Ji, H. L. (2018). Multiobjective optimization design and experimental study of desulfurization dust removal centrifugal pump based on immune particle swarm algorithm. *Advances in Materials Science & Engineering*, 2018(1), 1–10. <https://doi.org/10.1155/2018/6294824>
13. Noor, I., Qamar, I. (2021). Simulation of internal flow field of pitot-tube jet pump. *International Journal of Aerospace and Mechanical Engineering*, 15(2), 102–106.
14. Shigemitsu, T., Nakaishi, E., Maeda, M., Araki, Y. (2021). Influence of blade number on performance and internal flow condition of centrifugal pump for low viscous fluid food. *International Journal of Fluid Machinery and Systems*, 14(1), 132–141. <https://doi.org/10.5293/IJFMS.2021.14.1.132>
15. Tanaka, T., Toyomoto, T., Nasu, K., Tabaru, M. (2021). Transient characteristics of a centrifugal pump at rapid startup. *Journal of Physics: Conference Series*, 1909(1), 012032. <https://doi.org/10.1088/1742-6596/1909/1/012032>
16. Khoeini, D., Tavakoli, M. R. (2018). The optimum position of impeller splitter blades of a centrifugal pump equipped with vaned diffuser. *FME Transactions*, 46(2), 205–210. <https://doi.org/10.5937/fmet1802205K>
17. Mousmoulis, G., Kassanos, I., Aggidis, G., Anagnostopoulos, I. (2021). Numerical simulation of the performance of a centrifugal pump with a semi-open impeller under normal and cavitating conditions. *Applied Mathematical Modelling*, 83(3), 1814–1834.
18. Sugiyama, D., Ichinose, A., Takeda, T., Miyagawa, K., Negishi, H. et al. (2021). Investigation of internal flow in centrifugal pump diffuser using laser doppler velocimetry (LDV) and computational fluid dynamics. *Journal of Physics: Conference Series*, 1909(1), 1–10. <https://doi.org/10.1088/1742-6596/1909/1/012075>
19. Kim, S. J., Suh, J. W., Yang, H. M., Park, J., Kim, J. H. (2022). Internal flow phenomena of a pump-turbine model in turbine mode with different thoma numbers. *Renewable Energy*, 184(3), 510–525. <https://doi.org/10.1016/j.renene.2021.11.101>

20. Hosotani, T., Shigemitsu, T., Kawaguchi, Y., Inamoto, T., Ishiguro, T. et al. (2021). Influence of meridional plane shape on performance and internal flow of high head contra-rotating small hydroturbine. *Journal of Physics: Conference Series*, 1909(1), 1–8. <https://doi.org/10.1088/1742-6596/1909/1/012044>
21. Matsumoto, R., Kainuma, S., Toda, K., Yoshioka, D., Sawa, Y. (2021). Cool seal unit obstruction as an unusual cause of pump exchange of centrifugal pump EVAHEART. *Artificial Organs*, 45(7), 786–788. <https://doi.org/10.1111/aor.13902>
22. Wang, Y. Q., Ding, Z. W., Huo, X. W., Ji, H. L. (2018). Optimization design of centrifugal pump cavitation performance based on orthogonal test. *Journal of Shaoyang University (Natural Science Edition)*, 15(3), 26–33.
23. Liu, H. L., Tan, M. G. (2013). *Modern design methods for centrifugal pumps*. Beijing, China: China Machine Press.
24. Si, Q. R., Lin, G., Yuan, S. Q., Cao, R. (2016). Multi-objective optimization on hydraulic design of non-overload centrifugal pumps with high efficiency and low noise. *Transactions of the Chinese Society of Agricultural Engineering*, 32(4), 69–77.
25. Wei, X. L., Xue, B. J., Zhao, Q. (2010). Optimization design of the stability for the plunger assembly of oil pumps based on multi-target orthogonal test design. *Journal of Hebei University of Engineering (Natural Science Edition)*, 27(3), 95–99.